The Application of Taguchi Experiments in Developing Gecko-Inspired Dry Adhesive for Macro-Handling Applications

L. Nyanga[1], R.A. Govender[1*] & S. Matope[2]

ARTICLE INFO

Article details
Submitted by authors 11 Feb 2025
Accepted for publication 27 Nov 2025
Available online 12 Dec 2025

Contact details
* Corresponding author
reuben.govender@uct.ac.za

Author affiliations
1 Department of Mechanical Engineering, University of Cape Town, Cape Town, South Africa

2 Department of Industrial Engineering, Stellenbosch University, Stellenbosch, South Africa

ORCID® identifiers
L. Nyanga
https://orcid.org/0000-0002-7494-8860

R.A. Govender
https://orcid.org/0000-0002-1428-4142

S. Matope
https://orcid.org/0000-0001-5598-1027

DOI
http://dx.doi.org//10.7166/36-4-3193

ABSTRACT

Synthetic dry adhesives have been developed to mimic the gecko's adhesion using lithography and micro-machining of a mould to cast a suitable elastomer. Previous international studies used nano-manufacturing processes, which are expensive and are not readily available in South Africa. In this study, a simple micro-machining method was used using a three-axis milling machine and Vytaflex 30 to develop an adhesive pad. The Taguchi method to design experiments was used to determine the optimum machining conditions to create micro-wedges. The results show that, although a maximum adhesion pressure of 1,924 Pa was obtained with a preload pressure of 1,323 Pa, the adhesion force produced might not be suitable for macro-handling applications.

OPSOMMING

Sintetiese droë kleefmiddels is ontwikkel om 'n geitjie-toon se kleefvermoë na te boots deur litografie en mikro-bewerking gevolg deur gietvorm te gebruik. Die toerusting en materiaal wat in hierdie vervaardigingsprosesse gebruik word, is duur, en is meesal nie in Suid-Afrika beskikbaar nie. In hierdie studie word 'n eenvoudige mikro-bewerkingsmetode gebruik met behulp van 'n drie-as freesmasjien en Vytaflex 30 om 'n kleefblokkie te ontwikkel. Taguchi DOEs word gebruik om die optimale bewerkingstoestande te bepaal om mikrowiggies te skep. Die resultate toon dat, alhoewel 'n maksimum adhesiedruk van 1,924 Pa verkry is met 'n voorlaaidruk van 1,323 Pa, die adhesiekrag wat geproduseer word dalk nie geskik is vir makrohanteringstoepassings nie.

1. INTRODUCTION

Dry adhesives developed for robotic applications have an edge over other adhesion techniques such as magnetic attraction, suction, and grasping. Some of the advantages that dry adhesives have are that (1) they can adhere to different types of materials without needing an external source power; (2) they can be designed to be anisotropic; (3) they are easily removed by peeling rather than pulling off, which reduces energy requirements and simplifies the adhesion and detachment process; (4) they have high pull-off adhesion at lower preload force; and (5) the adhesive is not activated when no load is applied [1]. These dry adhesives are inspired by the Tokay gecko, which can climb vertical and inverted walls at high speed. To mimic the gecko's dry adhesion, researchers have developed different microstructures similar to gecko toe pads, such as nano bumps, nanopillars, mushroom tips, spatula tips, and micro-wedges [2]-[4]. Dry adhesives with mushroom and spatula tips have high adhesive strength; however, they also require a high detachment force owing to the symmetry of the tips [5]-[9]. This reduces the speed of operation and the applicability of grippers and robot feet. In contrast, micro-wedges have anisotropic adhesive characteristics that play a crucial role in their use because of the asymmetric shape of their tips. This makes it easy to turn the adhesion on and off. The preload required for attaching an anisotropic pad is less than the force required to detach it from the surface [10]-[11].

Several definitions can be found in the literature to characterise macro-handling. In this paper, macro-handling is defined as the location and transportation of parts greater than a few centimetres to metres. Meso-handling focuses on parts that are a few centimetres to fit in a box of 200 x 200 x 200 mm^3, while micro-handling handles parts that are 1 μm to 10 mm [12]-[14].

Although dry adhesives with micro-wedges are effective, their fabrication is still expensive. Micro-wedge machining requires high-tech CNC machines and specific formulations of PDMS elastomer, which is not readily available in South Africa. In this research, we used a simple micromachining method involving a three-axis milling machine and Vytaflex 30 urethane elastomer, which is readily available in South Africa, to create a dry adhesive. The Taguchi design of experiments was used to determine optimal machining conditions for the machining of the micro-wedges that would be required to mould the adhesive pad. The desired adhesive pad should be able to hold weight with a pressure of 3,000 Pa in an inverted position at a preload adhesion pressure of less than 1,500 Pa.

2. LITERATURE REVIEW

2.1. Gecko foot adhesion

A gecko foot consists of four structures: the soft skin on the flexible skin skeleton on the macroscale (shown in Figure 1A), *lamella* on the millimetre scale (shown in Figure 1B), micro-hairs called *setae* on the micrometre scale (shown in Figure 1C), and spatula-shaped *spatulae* that induce Van der Waal forces on the nanometre scale (shown in Figure 1D). With about 5,000 *setae* per square millimetre and each *seta* producing an average adhesion force and stress of 20 µN and 0.1 N/mm^2 respectively, the gecko foot can produce around 10 N with about 100 mm^2 pad area [15].

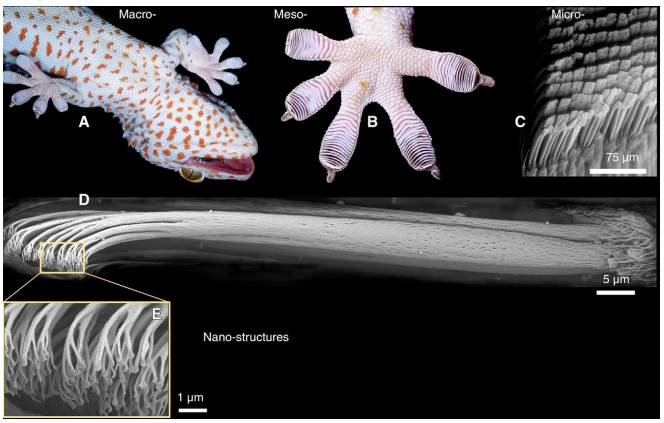

Figure 1: Structural hierarchy of the gecko adhesive system [16]

The hierarchical structure of the gecko foot increases the effective adhesion energy during detachment from a rough surface by increasing the elastic deformation energy [16]. It also increases the self-cleaning ability of gecko [17].

2.2. Synthetic dry adhesives

Dry adhesives can be classified according to the complexity and length scales of their surface features. The simplest grouping is plain dry adhesives, which grow in complexity to single-layer fibrillar adhesives; hierarchical fibrillar adhesives are the most complex, with features on multiple length scales [12].

2.2.1. Plain dry adhesives

Plain dry adhesives have smooth surfaces without fibrils or micro-wedges. They are usually created from polydimethylsiloxane (PDMS) and polyurethane elastomers, mainly the different variants of Vytaflex (10, 20, 30, 40, 60) [13]-[14]. These are the simplest pads to produce, as they are fabricated by mixing the resin and hardener, pouring the mixture into a mould, and letting it cure before demoulding the dry adhesive. These pads lack anisotropic characteristics, which means that a very high energy is required to detach them[18]-[20]. To use these pads effectively, the preload force and the adhesive force should be the same [21]-[24].

2.2.2. Single-layer fibrillar adhesives

Single-layer fibrillar adhesives contain only one fibril length scale, whereas hierarchical fibrillar adhesives contain two or more fibril length scales[12]. Single-layer fibrillar adhesives have been produced with vertical nano-pillars, polymer micro-pillars, wedge-shaped polymer microstructures, polypropylene nano-fibres, micro-pillars with triangular cross sections, hierarchical nano-pillars, hierarchical micro-pillars, micro-pillars with mushroom tips, and angled micro-pillars with angled mushroom tips [3],[4],[10]. Fabrication methods for single-layer fibrillar adhesives include moulding with nanoindentations and nanoporous filters. These methods require expensive and specialised equipment, such as producing dimples using an atomic force microscope (AFM) [25], creating pores between 0.3 and 2.5 μm on polycarbonate[26], using deep reactive ion etching and the notching effect [27], moulding PDMS on photolithographic templates [28], using ultraviolet-assisted capillary force lithography (CFL)[29], and using micromachining processes[30].

2.2.3. Hierarchical fibrillar adhesives

Hierarchical fibrillar adhesives are closest to the gecko adhesive, with a structured hierarchy of fibrils. They have been used in the creation of adhesive pads [29],[31],[32], grippers [17] and gecko robots [33],[35]. The techniques used in creating hierarchical fibrillar adhesives include chemical vapour deposition (CVD)[36], growing organoids on compliantly supported silicon dioxide platforms [37], soft moulding on photolithographic templates containing hierarchical holes [28], rapid prototyping [32], using a two-step UV-assisted capillary moulding with soft UV-curable polyurethane acrylate (PUA) [29] and using heated rollers and a sacrificial template[38].

2.3. Micro-wedges

Dry adhesives with micro-wedges have been developed to reduce the cost and time of producing fibrillar adhesives. These adhesives have high levels of adhesion produced from low preload forces [33],[34],[39], enable rapid attachment and detachment with minimal interaction forces between adhesion and grasped surface, and can be reused over a longer period than other types of dry adhesive [43]. The early versions of dry adhesives with micro-wedges were created by exposing SU 8 photoresist to multiangle UV light [24]. A cheaper and faster method to create micro-wedges that involved the micro-machining of sheet wax was developed by Day *et al*. [11]. Sylgard 170 PDMS was then used to create a dry adhesive in a mould that had the micro-wedges. Although the method proposed by [10] is cheaper than the previous methods used, it still requires specially shaped microtome blades for the machining process and laser profilometry to measure the depth of the wedges.

2.4. Taguchi method

The Taguchi method can be used to optimise the function of a product or process while minimising the resources used in the process of optimisation. The focus of the Taguchi method is to design a product/process that is insensitive to or robust in uncontrollable or noise parameters, while being aware of the controllable parameters that drive product performance. The effect of the noise parameters can be controlled at the design and development stage of the product or process, but cannot be eliminated; thus, the robust design in the Taguchi method seeks to minimise the effect of the noise parameters. The relationship between the control parameters and noise factors is not linear, and, to reduce variability in the product /process, the levels of control parameters that result in a small variation from the target in the response of the product/process to the noise factors have to be determined. The product/process is designed around those levels [40].

The three steps of system design, parameter design, and tolerance design are proposed to determine the control parameters and their levels. In the system design stage, scientific, engineering, and prior experiential knowledge are used to identify the control parameters and levels for the product and process to meet its intended purpose. In the parameter design, the optimum levels for the controllable system parameters are determined that produce less effect on the performance of the product when there are changes in the noise factor levels. Orthogonal arrays from the design of experiments theory are used to study many variables with a small number of experiments. The orthogonal-based approach simulation evaluates the mean and variance of the product's response caused by the variations in the noise factors. The signal-to-noise ratio (S/N) is then used to determine the optimum settings of the controllable parameters, as it incorporates the variation in the response variable and the desired target value. The analysis of variance (ANOVA) is carried out to determine the significant control factors. Tolerance design is only implemented if the parameter design is not sufficient to reduce the output variation [41],[42]. In this research, the Taguchi method to design experiments and ANOVA were used to investigate which of the design and manufacturing parameters strongly influenced the adhesive force of polyurethane dry adhesive pads.

3. METHODOLOGY

In this research, dry adhesives with micro-wedges were created using the method proposed by Day *et al.*[11]. These could be used as single-layer fibrillar adhesives when directly attached to the foot, or as hierarchical fibrillar adhesives when part of a foot attachment hierarchy. In this research, the mould for casting the polyurethane dry adhesive pad was manufactured with machined wax with wedges at the bottom. The desired adhesion pad should have an adhesion force higher than the preload force at a minimum preload pressure.

3.1. Sheet wax machining

The general setup for the machining of micro-wedges in the mould is shown in Figure 2. Freeman's sheet wax was melted in a mould box with the dimensions 200 x 80 x 50 mm in a furnace and left to cool down overnight. The lateral faces of the mould box were removed to allow access to mill the wax until its height was 5 mm; it was then clamped to the working table of the milling machine. To compensate for insufficient degrees of freedom on a three-axis milling machine worktable, the mould box was clamped at an incline to the milling worktable using fixtures to set the desired cutting angle. A cutter was created using a 60 mm-wide high-profile disposable microtome blade with a cutting angle of 35 °. The spindle was locked so that it did not rotate, but could only move in upward and downward motions. The wedge machining parameters are indicated in Figure 3, where θ_c is the cutting angle, d_c is the cutting depth, x_c is the wedge pitch distance, and β_c is the mould box holder inclination angle.

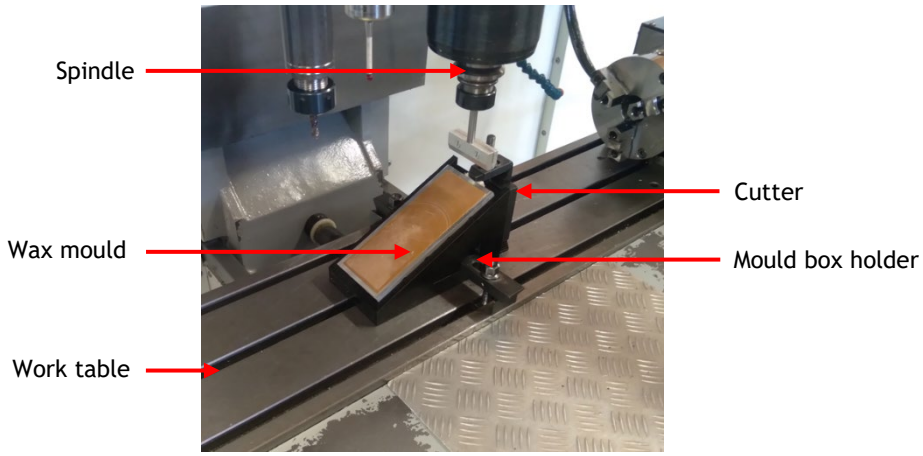

Figure 2: Wax-machining setup

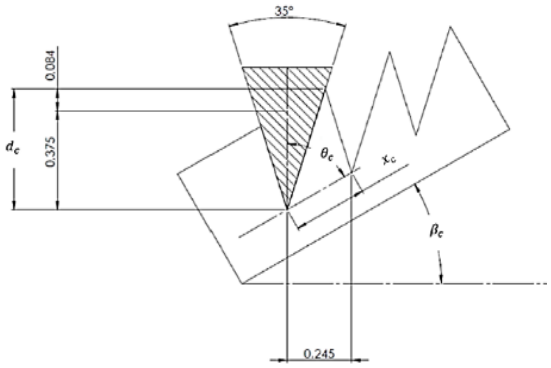

Figure 3: Wedge machining parameters

3.2. Taguchi design of experiments

The Taguchi method determines the optimal machining conditions for machining wedges with the equipment that is available. The effects of the input factors (cutting angle, cutting depth, feed rate, and type of lubricant) were investigated at three levels using the design of experiments (DOE). A four-three-level factors (L9) orthogonal array with the factors and levels is shown in Table 1. The full orthogonal array selected for the design of experiments is shown later in Table 2, alongside a summary of the adhesion pressure results.

Table 1: Factors and levels used in the experiment

Factor	Level		
	1	2	3
Cutting angle (°)	25	30	35
Cutting depth (mm)	0.1	0.3	0.5
Feed rate (mm/min)	150	200	250
Lubricant	No lubricant	Water	10% dishwasher

The Taguchi DOE creates a robust process design by identifying the control factors that reduce the variation in the process by minimising noise factors. This is achieved by implementing a two-step optimisation process that identifies the control factors that reduce process variation and those that have less or no effect on the S/N ratio. The S/N ratio measures the response variation of the target value under certain noise conditions. The “larger is better” signal ratio was used in analysing the results. The formula for calculating the “larger is better” S/N ratio is given as:

$$\frac{S}{N} = -10 * log\left(\frac{\sum(1/y^2)}{n}\right)$$

where y is the outcome of each experiment and n is the number of replications of each experiment.

3.3. Adhesive pad preparation

Vytaflex 30 was mixed with a 1:1 resin and hardener ratio to create the adhesive pads, and poured into the moulds with machined wax at the bottom. The filled moulds were degassed in a vacuum chamber. As this vacuum chamber could only achieve 75 kPa vacuum, degassing ran for two minutes. Initial attempts showed that the resin did not fully penetrate to the tip of the wedges owing to reliance on gravity filling, the viscosity of the resin, and the accumulation of the mould release agent (Mann 200 Ease Release). A test without mould release agent showed that the cast polyurethane could be removed from the mould without difficulty, but that it still lacked complete resin penetration. Consequently, a custom centrifuge was developed that allowed the moulds to be spun for two minutes to encourage resin penetration to the tip of the wedge cavities. The moulds were left to cure at room temperature overnight before being demoulded. The adhesive pad produced is shown in Figure 5.

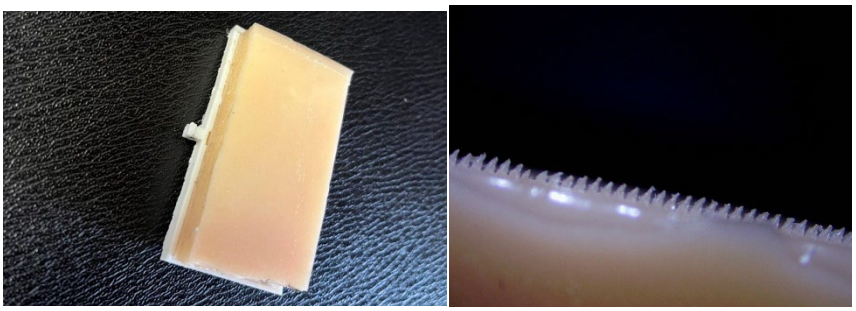

Figure 4: (a) Adhesive pad (b) Wedges on the adhesive pad

3.4. Adhesion force measurement

The adhesive pads were cut into 60 x 30 mm rectangular pads. To measure the adhesion force produced by the adhesive pad, the force measurement jig shown in Figure 4 was manufactured. A servo motor controls the actuating arm through a lead screw. The force exerted on the glass plate is measured with a 1kg beam load cell, which is captured via the Arduino used to control the lead screw motor. The load cell data from the Arduino is captured on the PC using CoolTerm software. The jig is calibrated in grams to simplify its calibration, as the weights used for calibration are in grams. A sample of preload and adhesion force measurement calibrated in grams and obtained from the jig is shown in Figure 5. The preload values are positive, while the adhesion values are negative. The adhesion pressure is assumed to be uniformly distributed and is calculated from the pressure obtained from the measuring jig using the formula:

$$P = \frac{mg}{A} = \frac{(m * 9.81)/1000}{(0.06 * 0.03)} = 5.4m\ Pa$$

Here, m is the mass reading from the measuring jig, g is the gravitational acceleration, and A is the cross-sectional area of the dry adhesive in contact with the glass surface.

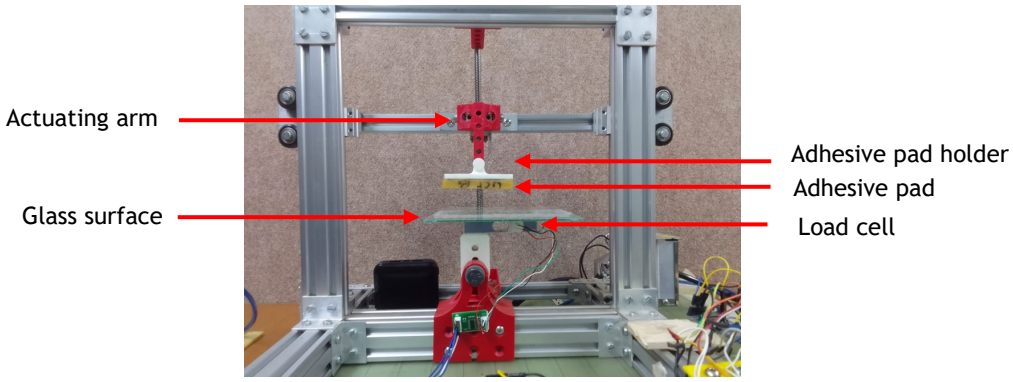

Figure 5: Adhesion force measurement jig

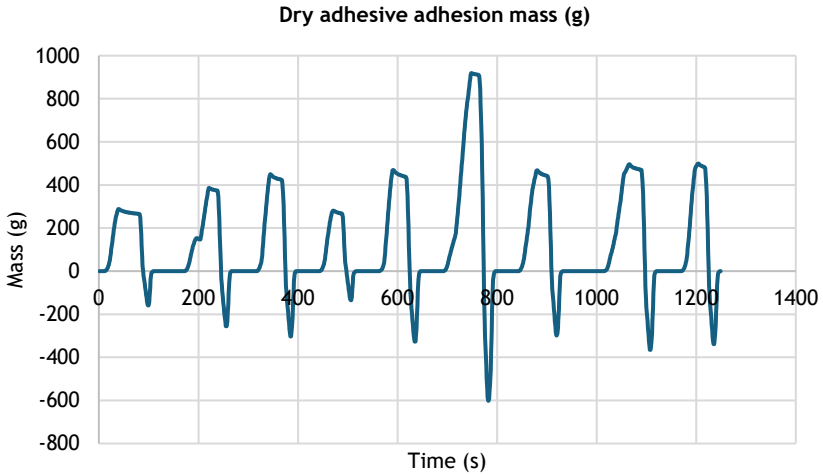

Figure 6: Measurement of adhesion force

4. RESULTS AND ANALYSIS

The results of the average adhesion pressure obtained from the Taguchi DOE are shown in Table 2. The adhesion pressure of Vytaflex 30 on a smooth surface is obtained from the function [24]:

$$P_a = AP_p^B$$

where P_a is the adhesion pressure, P_p is the preload pressure, and A and B are determined in experiments by measuring the adhesive pressure at different preload pressures. When two corresponding preloads pressure and adhesion pressure points (P_{a1} , P_{p1} and P_{a2} , P_{p2}) are considered, A and B can be calculated as follows:

$$B = \frac{\ln P_{a2} - \ln P_{a1}}{\ln P_{p1} - \ln P_{p2}}$$

$$B = e^{(\ln P_{a1} - B \ln P_{p1})}$$

Table 2: L9 orthogonal array

	Independent variables				Dependent variable		
Trial	Cutting angle (°)	Cutting depth (mm)	Lubricant	Feed rate (mm/min)	R1 (Pa)	R2 (Pa)	R3 (Pa)
1	25	0,1	No_lubricant	150	244,92	234,40	204,59
2	25	0,3	Water	200	508,10	462,76	527,23
3	25	0,5	Dishwasher	250	1 978,24	1 838,29	1 954,37
4	30	0,1	Water	250	322,91	278,00	258,93
5	30	0,3	Dishwasher	150	119,63	535,46	561,51
6	30	0,5	No_lubricant	200	785,35	170,75	152,22
7	35	0,1	Dishwasher	200	151,73	769,92	746,27
8	35	0,3	No_lubricant	250	184,32	144,86	238,49
9	35	0,5	Water	150	532,57	480,96	561,51

To obtain uniform results, a preload adhesion of 1 363 Pa (250g) was used to measure the adhesion pressure of all the pads. R1, R2, and R3 in Table 1 are the calculated adhesion pressures from the experiment's repetition. A maximum adhesion pressure of 1 924 Pa was attained when the cutting angle was 25 °, the cutting depth was 0.5 mm, the feed rate was 250 mm/min, and a 10% Sunlight dishwashing liquid solution was used as a lubricant.

Minitab was used to determine the responses for the means and S/N ratios and to conduct the ANOVA. The generic L9 factor levels 1,2, and 3 were used to feed the information into Minitab, with the lubricant levels being the ability of the lubricant to remove the wax from the cutter or to keep the wax from sticking to the cutter – i.e., no_lubricant (1), water (2) and dishwasher (3). The variations of the means in Figure 6 indicate that the differences between the maximum and minimum average response for cutting angle, cutting depth, lubricant and feed rate were 529.8, 582.5, 699.5, and 413.6, respectively. This shows that the factor that affected the adhesion pressure the most was the type of lubricant used, followed by the cutting depth, cutting angle, and feeding rate. Generally, when the response to means is considered, half of the total degrees of freedom in the orthogonal array are used to determine the optimum conditions. In the experiments, an L9 orthogonal array was used, which has 8 degrees of freedom. Half of the degrees of freedom would result in the top four factors being selected. The experiment already had four factors, which meant that all four factors were important. Using the response for the means is considered an easy analysis, but does not consider the robustness of the process. Figure 6 was used to obtain the optimal levels based on the means that resulted in the optimal levels being a cutting angle of 25 °, a cutting depth of 0.5 mm, a 10% Sunlight liquid dishwashing liquid lubricant, and a feeding rate of 250 mm/min.

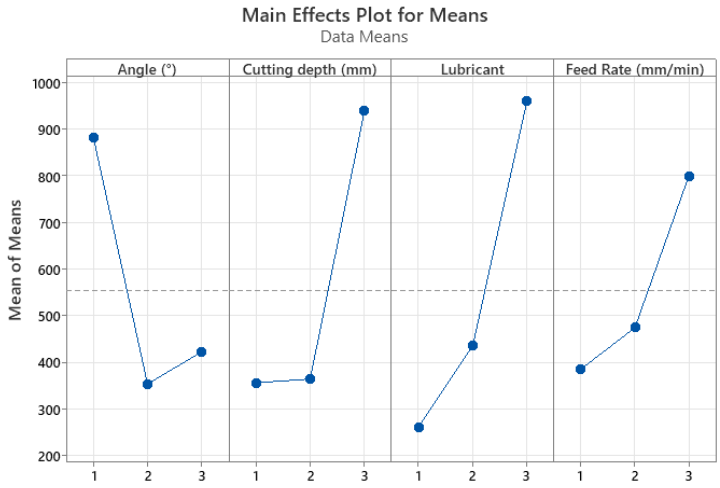

Figure 7: Main effects plot for means

To create a robust process, the variance of the "larger is better" S/N ratios was analysed and created. The results of the S/N ratios in Figure 8 indicated that the differences between the maximum and minimum average response for cutting angle, cutting depth, lubricant, and feed rate were 8.64, 7.21, 7.26, and 4.12 respectively. This indicated that the factor that affected the adhesion pressure the most was the cutting angle, followed by the type of lubricant used, the cutting depth, and the feed rate.

Figure 8: Signal-to-noise ratios

The results of the ANOVA showed the significant factors of the experiment when considering the P and F values. A factor is considered significant if the p-value is less than 0.05 and the F value is very high. It can be observed from Table 3 that all the P values were less than 0.05 and the F values were high, which made all the factors significant, as established by the response to the means and the S/N ratios. When considering the F values, the same conclusion on the rank of significance could be reached when the S/N values were used.

Table 3: ANOVA results

Source	DF	Adj SS	Adj MS	F-value	P-value
Cutting angle	2	1492052	746026	20,59	0,000
Cutting depth	2	2008814	1004407	27,72	0,000
Lubricant	2	2385533	1192766	32,92	0,000
Feed rate	2	853624	426812	11,78	0,001
Error	18	652181	36232		
Total	**26**	**7392204**			

5. DISCUSSION

The factors affecting the performance of the dry adhesives with micro-wedges can be discussed at the level of mould machining, as investigated by Day [11], and at the level of casting, which is influenced by the material used for the casting and the casting procedure.

Even though a maximum adhesion pressure of 1 924 Pa was obtained with a preload force of 1 323 Pa, the adhesion pressures obtained were lower than the targeted adhesion pressures. This made the dry adhesive pads that were developed unsuitable for macro-handling. To reach this scenario with the pads, the preload pressure had to be increased to 4 905 Pa (900g on the test bench). Further optimisation of the geometric variables investigated here might not yield the desired result. A contributor to the low adhesion force might be the stiffness of the elastomer, as Vytaflex 30 has a shore hardness of 30A. A material with lower stiffness, such as Vytaflex 10, would have to be investigated in future.

Although the table of response for means results shows that the process was more sensitive to lubricant, cutting, and cutting depth, with the level of sensitivity decreasing respectively, the table of S/N ratios shows that the process was more sensitive to the cutting angle, type of lubricant, cutting depth, and feed rate. These results are consistent with the observation made by Day [11]. The cutting angle affected the shape of the neighbouring cavities during machining, which then affected the shape of the wedges produced in the dry adhesive. The sensitivity to the lubricant was attributed to wax build-up on the cutter, depending on the lubricant used, which distorted the shape of the next wedges being cut. The dishwashing solution either removed or avoided wax build-up on the cutter. The depth of the cut would influence the shape of the wedges on the dry adhesive. If the depth were small and the material used for casting were less viscous, the wedges would not be well defined, resulting in less adhesion force. The lower sensitivity to the feed rate was expected, as the wax was a soft material.

Generally, micro-machining wax using a three-axis milling machine is not as accurate as when a six-axis milling machine is used, but it can be used as a compromise when a six-axis milling machine is unavailable. This could be achieved by using attachments on the machine table to compensate for the loss of axes. The other change faced with the milling machine used was the lack of a closed-loop control when measuring the depth of micro-wedges and the pitch of the wedge crests. Since there was no way to measure during machining, the measurements were set into the machining programme, which was not always the best, given the size of the wedges that were supposed to be machined. The Taguchi DOE enables one to optimise a process with many factors that can be run at different levels. The process is economical because the number of possible experiments is reduced by using orthogonal arrays. The process developed in this paper sought to develop a robust design in machining the wedges so that, once the optimum inputs had been established, the process would give the required result even without the way to measure the size of the wedges during machining.

The type of material used to cast the adhesive pads would need further investigation. A PDMS material, such as Sylgard 170, was used in previous investigations, but because of the unavailability of this Sylgard product in South Africa, Vytaflex 30 was used as a substitute, even though the materials belong to different groups and behave differently. One of the main drawbacks of using urethane rubber to cast micro-wedges is that it sticks to the mould and wedges more than silicone does. This results in the urethane ripping the wedges on the wax during demoulding, which results in the adhesive pad being less effective, as was observed with the adhesion pressure being less than the preload pressure. The use of a softer material, such as Vytaflex 10, which is not readily available in South Africa but that can be imported through distributors, should be investigated.

6. CONCLUSION

Dry adhesives that mimic the gecko foot have been produced using expensive processes such as lithography and micro-machining using high-tech milling machines. In the case when this type of machinery is not available, the Taguchi method can be used to optimise the machining of micro-wedges with low-tech machinery. Micromachining the wedges can be achieved, but the adhesion pads created with Vytaflex 30 are not suitable for macro-handling with a preload adhesion pressure of 1 363 Pa. A material with a lower shore hardness would have to be investigated.

REFERENCES

[1] **Autumn, K., Niewiarowski, P. H., & Puthoff, J. B.** 2014. Gecko adhesion as a model system for integrative biology, interdisciplinary science, and bioinspired engineering. *Annual Review of Ecology, Evolution, and Systematics*, 45(1), 445–470. https://doi.org/10.1146/annurev-ecolsys-120213-091839

[2] **Sitti, M., & Fearing, R.** 2002. Nanomolding-based fabrication of synthetic gecko foot hairs. *Proceedings of IEEE-NANO 2002*, 137–140.

[3] **Menguc, Y.** 2012. Gecko-inspired, controlled adhesion and its applications. PhD dissertation, Carnegie Mellon University, Pittsburgh, PA.

[4] **Murphy, M. P., Aksak, B., & Sitti, M.** 2009. Gecko-inspired directional and controllable adhesion. *Small*, 5, 170–175.

[5] **Gorb, S., Varenberg, M., Peressadko, A., & Tuma, J.** 2007. Biomimetic mushroom-shaped fibrillar adhesive microstructure. *Journal of the Royal Society Interface*, 4, 271–275.

[6] **Aksak, B., Murphy, M.P., & Sitti, M.** 2007. Adhesion of biologically inspired vertical and angled polymer microfiber arrays. *Langmuir*, 23(6), 3322-3332.

[7] **Sameoto, D., Sharif, H., & Menon, C.** 2012. Investigation of low-pressure adhesion performance of mushroom shaped biomimetic dry adhesives. *Journal of Adhesion Science and Technology*, 26, 2641–2652.

[8] **Seo, S. Lee, J., Kim, K. S., Ko, K. H., Lee, J. H., & Lee, J.** 2014. Anisotropic adhesion of micropillars with spatula pads. *ACS Applied Materials & Interfaces*, 6, 1345–1350.

[9] **Varenberg, M., Pugno, N. M., & Gorb, S. N.** 2010. Spatulate structures in biological fibrillar adhesion. Soft *Matter*, 6, 3269–3272.

[10] **Parness, A., Soto, D., Esparza, N., Gravish, N., Wilkinson, M., Autumn, K., & Cutkosky, M.** 2009. A microfabricated wedge-shaped adhesive array displaying gecko-like dynamic adhesion, directionality and long lifetime. *Journal of the Royal Society Interface*, 6(41), 1223–1232. https://doi.org/10.1098/rsif.2009.0048

[11] **Day, P., Eason, E. V., Esparza, N., Christensen, D., & Cutkosky, M.** 2013. Microwedge machining for the manufacture of directional dry adhesives. *Journal of Micro and Nano-Manufacturing*, 1(1), 011001. https://doi.org/10.1115/1.4023161

[12] **Sanchez-Salmeron, A. J.** 2005. Recent development in micro-handling systems for micro-manufacturing. *Journal of Materials Processing Technology*, 167(2-3), 499-507. DOI: 10.1016/j.jmatprotec.2005.06.027

[13] **Sanchez-Salmeron, A. J.** 2010. Handling for micro-manufacturing. In *Micromanufacturing engineering and technology*, ch. 18. Burlington, NJ: Elsevier Science.

[14] **Read, S., Van der Merwe, A. Schutte, C. S., Matope, S., & Mueller, M.** 2012. Development of a micro material handling system. *Proceedings of the International Conference on Computers and Industrial Engineering, CIE42*, Cape Town, South Africa.

[15] **Autumn, K., Liang, Y. A., Hsieh, S. T., Zesch, W., Chan, W. P., Kenny, T. W., Fearing, R. & Full, R. J.** 2000. Adhesive force of a single gecko foot-hair. *Nature*, 405, 681–685. https://doi.org/10.1038/35015073.

[16] **Autumn, K.** 2006. Properties, principles, and parameters of the gecko adhesive system. In A. Smith & J. Callow (eds.), *Biological adhesives*. Berlin, Heidelberg: Springer, pp. 225–256.

[17] **Gao, H. J., Wang, X., & Yao, H. M.** 2005. Mechanics of hierarchical adhesion structures of geckos. *Mechanics of Materials*, 37, 275–285.

[18] **Tian, Y., Wan, J., Pesika, N., & Zhou, M.** 2013. Bridging nanocontacts to macroscale gecko adhesion by sliding soft lamellar skin supported setal array. *Scientific Reports*, 3, 1382. https://doi.org/10.1038/srep01382

[19] **Li, Y., Krahn, J., & Menon, C.** 2016. Bioinspired dry adhesive materials and their application in robotics: A review. *Journal of Bionic Engineering*, 13(2), 181–199. https://doi.org/10.1016/S1672-6529(16)60293-7

[20] **Cronje, G., & Matope, S.** 2015. Polyurethane grippers as a substitute for vacuum grippers: A case study in an electronics environment. *7th International Conference on Latest Trends in Engineering & Technology (ICLTET'2015)*, 125–128. https://doi.org/10.15242/iie.e1115034

[21] **Menon, C., Murphy, M., & Sitti, M.** 2004. Gecko inspired surface climbing robots. *2004 IEEE International Conference on Robotics and Biomimetics*, 431–436. https://doi.org/10.1109/ROBIO.2004.1521817

[22] **Chu, Z., Wang, C., Hai, X., Deng, J., Cui, J., & Sun, L.** 2019. Analysis and measurement of adhesive behavior for gecko-inspired synthetic microwedge structure. *Advanced Materials Interfaces*, 6(12). https://doi.org/10.1002/admi.201900283

[23] **Li, Y., Sameoto, D., & Menon, C.** 2009. Properties validation of an anisotropic dry adhesion designed for legged climbing robots. *2009 IEEE International Conference on Robotics and Biomimetics (ROBIO)*, 1906-1911.

[24] **Liu, Y., Kim, H., & Seo, T.** 2016. AnyClimb: A new wall-climbing robotic platform for various curvatures. *IEEE/ASME Transactions on Mechatronics*, 21(3), 1812–1821. https://doi.org/10.1109/TMECH.2016.2529664

[25] **Geim, A. K., Dubonos, S. V., Grigorieva, I. V., Novoselov, K. S., Zhukov, A. A., & Shapoval, S. Y.** 2003. Microfabricated adhesive mimicking gecko foot-hair. *Nature Materials*, 2(7), 461–463. https://doi.org/10.1038/nmat917

[26] **Majidi, C., Groff, R., Maeno, Y., Schubert, B., Baek, S., Bush, B., Maboudian, R., Gravish, N., Wilkinson, M., Autumn, K., & Fearing, R.** 2006. High friction from a stiff polymer using microfiber arrays. *Physical Review Letters*, 97(7), 18–21.

[27] **Kim, S., Aksak, B., & Sitti, M.** 2007. Enhanced friction of elastomer microfiber adhesives with spatulate tips. *Applied Physics Letters*, 91, 221913.

[28] **Greiner, C., Arzt, E., & Del Campo, A.** 2009. Hierarchical gecko-like adhesives. *Advanced Materials*, 21, 479–482.

[29] **Jeong, H. E., Lee, J. K., Kim, H. N., Moon, S. H., & Suh, K. Y.** 2009. A nontransferring dry adhesive with hierarchical polymer nanohairs. *Proceedings of the National Academy of Sciences of the United States of America*, 106(14), 5639–5644. https://doi.org/10.1073/pnas.0900323106

[30] **Kwak, M. K., Jeong, H. E., Bae, W. G., Jung, H.-S., & Suh, K. Y.** 2011. Anisotropic adhesion properties of triangular-tip-shaped micropillars. *Small*, 7, 2296–2300.

[31] **Lee, D. Y., Lee, D. H., Lee, S. G., & Cho, K.** 2012. Hierarchical gecko-inspired nanohairs with a high aspect ratio induced by nanoyielding. *Soft Matter*, 8(18), 4905–4910. https://doi.org/10.1039/c2sm07319f

[32] **Murphy, M. P., Kim, S., & Sitti, M.** 2009. Enhanced adhesion by gecko-inspired hierarchical fibrillar adhesives. *ACS Applied Materials and Interfaces*, 1(4), 849–855. https://doi.org/10.1021/am8002439

[33] **Seo, J., Eisenhaure, J., & Kim, S.** 2016. Micro-wedge array surface of a shape memory polymer as a reversible dry adhesive. *Extreme Mechanics Letters*, 9, 207–214. https://doi.org/10.1016/j.eml.2016.07.007

[34] **Kim, S., Spenko, M., Trujillo, S., Heyneman, B., Santos, D., & Cutkoskly, M. R.** 2008. Smooth vertical surface climbing with directional adhesion. *IEEE Transactions on Robotics*, 24(1), 65–74. https://doi.org/10.1109/TRO.2007.909786

[35] **Kim, S., Spenko, M., Trujillo, S., Heyneman, B., Mattoli, V., & Cutkosky, M. R.** 2007. Whole body adhesion: Hierarchical, directional and distributed control of adhesive forces for a climbing robot. *2007 IEEE International Conference on Robotics and Automation*, 1268–1273.

[36] **Hu, S., Xia, Z., & Dai, L.** 2013. Advanced gecko-foot-mimetic dry adhesives based on carbon nanotubes. *Nanoscale*, 5(2), 475–486. https://doi.org/10.1039/c2nr33027j

[37] **Northen, M. T., & Turner, K. L.** 2006. Meso-scale adhesion testing of integrated micro- and nano-scale structures. *Sensors and Actuators A: Physical*, 130–131(sp. iss.), 583–587. https://doi.org/10.1016/j.sna.2005.10.032

[38] **Lee, J., Bush, B., Maboudian, R., & Fearing, R. S.** 2009. Gecko-inspired combined lamellar and nanofibrillar array for adhesion on nonplanar surface. *ACS Publications*, 25(21), 12449–12453. https://doi.org/10.1021/la9029672

[39] **Santos, D., Spenko, M., Parness, A., Kim, S., & Cutkosky, M.** 2007. Directional adhesion for climbing: Theoretical and practical considerations. *Journal of Adhesion Science and Technology*, 21(12), 1317–1341.

[40] **Mitra, A.** 2011. The Taguchi method. *WIREs Computational Statistics*, 3(5), 472-480. https://doi.org/10.1002/wics.169

[41] **Unal, R. & Dean, E. B.** 1990. Taguchi approach to design optimisation for quality and cost: An overview. 1991 Annual Conference of the International Society of Parametric Analysts. https://ntrs.nasa.gov/citations/20040121019

[42] **Hamzaçebi, C.** 2020. Taguchi method as a robust design tool. In Li, P., Pereira, P. A. R., & Navas, H. (eds). *Quality control: Intelligent manufacturing, robust design and charts*. InTechopen, ch. 7. https://doi.org/10.5772/intechopen.94908

[43] **Cauligi, A., Chen, T. G., Suresh, S. A., Dille, M., Ruiz, R. G., Vargas, A. M., Pavone, M., & Cutkosky, M. R.** 2020. Design and development of a gecko-adhesive gripper for the Astrobee free-flying robot. *arXiv:2009.09151*.